

Time-Aware Attention for Enhanced Electronic Health Records Modeling

Junhan Yu^{1*}; Zhunyi Feng^{2*}; Junwei Lu³,
Tianxi Cai³, Doudou Zhou^{1†}

¹ Department of Statistics and Data Science, National University of Singapore

² School of Computing, National University of Singapore

³ Department of Biostatistics, Harvard T.H. Chan School of Public Health, USA

Abstract

Electronic Health Records (EHR) contain valuable clinical information for predicting patient outcomes and guiding healthcare decisions. However, effectively modeling Electronic Health Records (EHRs) requires addressing data heterogeneity and complex temporal patterns. Standard approaches often struggle with irregular time intervals between clinical events. We propose TALE-EHR, a Transformer-based framework featuring a novel time-aware attention mechanism that explicitly models continuous temporal gaps to capture fine-grained sequence dynamics. To complement this temporal modeling with robust semantics, TALE-EHR leverages embeddings derived from standardized code descriptions using a pre-trained Large Language Model (LLM), providing a strong foundation for understanding clinical concepts. Experiments on the MIMIC-IV and PIC dataset demonstrate that our approach outperforms state-of-the-art baselines on tasks such as disease progression forecasting. TALE-EHR underscores the benefit of integrating explicit, continuous temporal modeling with strong semantic representations provides a powerful solution for advancing EHR analysis.

1 Introduction

Deep learning approaches, particularly transformer-based architectures, have propelled significant advancements in natural language processing (NLP). Within healthcare, Electronic Health Records (EHRs) offer a rich repository of information, encompassing patient medical histories, diagnoses, laboratory results, and clinical notes. However, harnessing this data for predictive modeling remains challenging due to its fragmented, sensitive, and heterogeneous nature, alongside its crucial inherent temporal complexity. Accurately capturing

*Equal contribution.

†Corresponding author.

the sequence, timing, and duration between clinical events is paramount for understanding patient trajectories and predicting future outcomes.

Modeling the temporal structure of clinical events is essential. The sequence and precise timing of diagnoses, medications, and interventions carry vital information. Short intervals might indicate acute episodes, whereas longer intervals could reflect chronic condition management or latency periods. To address this critical temporal dimension, we introduce a novel time-aware attention mechanism. This mechanism moves beyond standard self-attention by explicitly incorporating the continuous temporal intervals between clinical events into the attention score calculation. This enables the Transformer model to dynamically weight the influence of past events based not only on their semantic similarity but crucially on their temporal proximity, thereby capturing both semantic content and the fine-grained temporal dynamics inherent in patient data.

Furthermore, Conventional EHR code embeddings often struggle with semantic nuances. LLMs pre-trained on textual code descriptions (Hur et al., 2022; Wang and Sun, 2022; Wang et al., 2024; Su et al., 2025) offer richer semantics, overcoming heterogeneity. We leverage this for robust code embeddings, enhancing performance even with limited data.

To integrate these insights, we propose the Time-Aware Language Encoder for EHR (TALE-EHR), a transformer-based point process framework. TALE-EHR’s core innovation lies in its time-aware attention mechanism, specifically designed for the irregularities of EHR event sequences. This is complemented by leveraging embeddings derived from clinical code descriptions via a pre-trained LLM, ensuring robust semantic understanding and facilitating better generalization across healthcare institutions with diverse coding practices. By processing the textual descriptions for 12,232 distinct medical codes within a temporally sophisticated architecture, TALE-EHR provides a comprehensive and interpretable representation of patient trajectories, leading to improved predictive performance.

Our key contributions are as follows. First, we design a novel time-aware attention mechanism that explicitly models continuous temporal intervals between clinical events within a Transformer framework, improving the capture of time-dependent relationships in EHR data. Second, we leverage pre-trained LLM embeddings derived from standardized code descriptions. This provides our model with strong initial semantic understanding, which, when combined with our temporal modeling, leads to enhanced representation robustness and improved predictive performance, particularly in handling diverse clinical codes. Third, our framework uniquely combines enhanced semantic understanding with explicit temporal dynamic modeling, offering a more holistic approach to EHR sequence analysis.

To empirically validate TALE-EHR’s effectiveness and generalizability, we conducted extensive experiments on two distinct EHR datasets: the large-scale MIMIC-IV database (Johnson et al., 2023) (over 360,000 adult patient records) and the Paediatric Intensive Care (PIC) database (Zeng et al., 2020). On MIMIC-IV, TALE-EHR achieves state-of-the-art performance in predicting next-visit medical events across all 12,232 unique codes in our processed dataset. Furthermore, it demonstrates robust prediction for specific diseases on MIMIC-IV, attaining an average Area Under the Curve (AUC) of 0.926 across these evaluated conditions. Complementary experiments on the PIC dataset further underscore our method’s effectiveness and robustness across different clinical settings and patient populations. These comprehensive evaluations highlight TALE-EHR’s capabilities, particularly its enhanced temporal modeling, across a variety of clinical prediction tasks.

2 Related Work

The representation of EHR for predictive modeling has been extensively studied, with approaches showing diverse strategies for capturing and utilizing the complex information within EHR data, particularly its temporal dynamics.

Early works employed RNNs and variants (Choi et al., 2016; Du et al., 2016; Shang et al., 2021) for sequential dependencies but faced limitations with long-range dependencies and temporal irregularities common in EHRs. Knowledge graph-guided (Zhang et al., 2019; Wang et al., 2020; Li et al., 2019) and contrastive learning (Shang et al., 2019) approaches have also been explored, yet often rely on curated structures or prioritize structured codes over nuanced temporal dynamics (Chen et al., 2020). Transformer-based models (Lee et al., 2020; Choi et al., 2020; Lample et al., 2019) excel at long-range dependencies, but effectively integrating temporal information specific to EHRs remains an active research area.

Recognizing temporal importance, studies have incorporated various strategies. Some focused on sequence order or semantic-based attention within RNNs (Choi et al., 2017; Ma et al., 2017), or combined RNNs with point process theory or time-aware gates (Du et al., 2016; Liu et al., 2019, 2022). Within Transformer architectures, approaches include hierarchical time-aware attention (Luo et al., 2020), discrete time tokens (Pang et al., 2021), standard time embeddings with specialized output layers (Steinberg et al., 2024), text serialization relying on positional embeddings (Lee et al., 2024), or retrieval-enhanced methods using event timestamps alongside embeddings (Kim et al., 2024).

While advancing the field, these methods often handle temporal information indirectly, e.g., via sequence order, separate time embeddings, discrete markers, or fixed structural integrations, potentially limiting direct, adaptive modulation by continuous temporal differences.

In contrast, TALE-EHR introduces a unique time-aware attention mechanism by directly incorporating a learnable temporal weighting function, $w(t)$, into the Transformer’s self-attention computation. This function dynamically adjusts attention scores based on the continuous time difference ($|t_j - t_k|$) between events. Unlike approaches relying primarily on sequence order, pre-fusing time embeddings, or using discrete markers, TALE-EHR’s $w(t)$ directly modulates semantic relevance by continuous time differences at the very moment of attention calculation. This allows for adaptive capture of complex temporal dependencies, promoting a deep fusion of semantic and temporal information for richer representations, rather than treating time as a preprocessing step or an auxiliary feature.

3 Method

EHR data contain rich temporal information that reflects patients’ clinical trajectories. We model this data as a *marked temporal point process*, where each patient i is represented by a sequence of time-stamped clinical events:

$$\mathcal{H}^{(i)} = \{(t_1^{(i)}, c_1^{(i)}), (t_2^{(i)}, c_2^{(i)}), \dots, (t_{m_i}^{(i)}, c_{m_i}^{(i)})\}$$

with $t_1^{(i)} \leq t_2^{(i)} \leq \dots \leq t_{m_i}^{(i)}$. Here, $t_j^{(i)}$ represents the timestamp of the j -th clinical event, $c_j^{(i)} \in \mathcal{C}$ with \mathcal{C} being the set of all possible EHR codes, and m_i is the total number of clinical events in the patient i .

Following the point process framework (Daley and Vere-Jones, 2003), let $N^{(i)}$ denote the counting process for patient i , defined by occurrence times $\{t_1^{(i)}, t_2^{(i)}, \dots\}$. For a time interval $A \subseteq \mathbb{R}^+$, we define $N^{(i)}(A) = |\{t_j^{(i)} : t_j^{(i)} \in A\}|$ as the number of events in A . The patient history up to time t is denoted as $\mathcal{H}_t^{(i)} = \{(t_j^{(i)}, c_j^{(i)}) : t_j^{(i)} \leq t\}$.

Additionally, each patient is assumed to have a demographic covariate vector $\mathbf{Z}_i(t) \in \mathbb{R}^p$, which includes both time-invariant covariates (e.g., sex and race) and time-varying covariates (e.g., age). Based on this, the conditional intensity function is formally defined as:

$$\lambda^{(i)}(t) = \lim_{dt \rightarrow 0} \mathbb{E}[N^{(i)}(dt) | \mathcal{H}_t^{(i)}, \mathbf{Z}_i(t)] / dt$$

where $N^{(i)}(dt) = N^{(i)}([t, t + dt])$ denotes the number of events occurring in the infinitesimal interval $[t, t + dt)$. The conditional intensity function $\lambda^{(i)}(t)$ describes the instantaneous rate at which events are expected to occur at time t , given the patient’s history $\mathcal{H}_t^{(i)}$ and covariates $\mathbf{Z}_i(t)$.

To operationalize this theoretical framework with modern deep learning, we implement the conditional intensity function using transformer-based architectures. Our model aims to achieve two key objectives: (1) Event Timing Prediction: the timing of future events is modeled by a parameterized intensity function:

$$\lambda^{(i)}(t) = g(\mathbf{Z}_i(t), \mathbf{h}_t^{(i)}); \tag{1}$$

and (2) Event Prediction: the type of the next clinical event is predicted via:

$$P(c_t | \mathbf{Z}_i(t), \mathcal{H}_t^{(i)}) = f(\mathbf{Z}_i(t), \mathbf{h}_t^{(i)}). \tag{2}$$

Here, c_t is the medical code for the next event after time t , $\mathbf{h}_t^{(i)}$ is a learned representation of patient history $\mathcal{H}_t^{(i)}$, and g and f are neural network functions.

The proposed TALE-EHR algorithm, as illustrated in Figure 1, leverages three core innovations to effectively model clinical event sequences. First, we introduce a time-aware attention mechanism that explicitly captures temporal relationships between events, enabling the model to effectively account for complex dependencies in patient histories (Section 3.1). Second, the framework incorporates multi-scale temporal features to handle patterns occurring across varying time scales, ensuring robust representation of both short-term and long-term dynamics (Section 3.2). Third, medical codes are embedded using pre-trained language models, providing a unified and interpretable representation of clinical events. We propose a joint training strategy that optimizes both timing and content prediction objectives (Section 3.3). This allows the model to generalize across a wide range of downstream clinical tasks (Section 3.4).

3.1 Time-aware Attention Mechanism

A core component of our approach is the time-aware attention mechanism, which explicitly captures temporal relationships between clinical events. Given the history \mathcal{H}_t (superscript (i) omitted for simplicity), each event is encoded through the attention mechanism as:

$$E_{c_j}(t) = \sum_{(c_k, t_k) \in \mathcal{H}_t} A(Q_{c_j}, K_{c_k}, |t_j - t_k|) V_{c_k}, \tag{3}$$

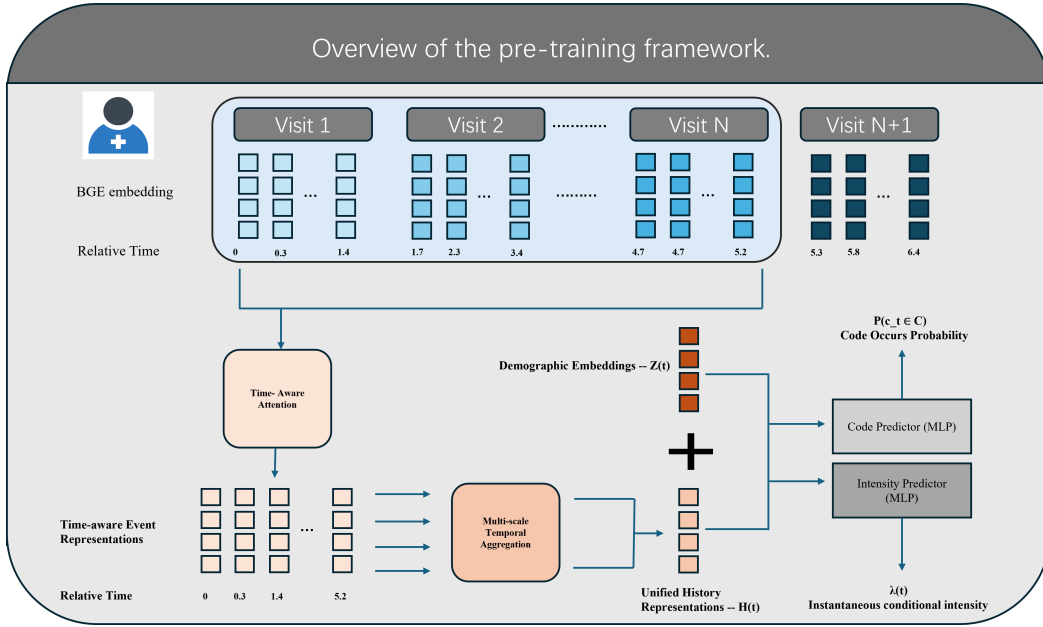


Figure 1: Overview of the TALE-EHR framework.

where $(c_j, t_j) \in \mathcal{H}_t$. To generate robust semantic embeddings (\mathbf{v}_c) for medical codes from their textual descriptions, we utilize BGE (Chen et al., 2024), a powerful general-purpose text encoder pre-trained on diverse, broad-domain corpora. This approach helps mitigate potential biases from medical-specific pre-training and enhances generalization. The query (Q_c), key (K_c), and value (V_c) vectors are then derived by applying separate multi-layer perceptrons (MLPs) to these pre-trained LLM embeddings \mathbf{v}_c , i.e., $Q_c = \text{MLP}_Q(\mathbf{v}_c)$, $K_c = \text{MLP}_K(\mathbf{v}_c)$, and $V_c = \text{MLP}_V(\mathbf{v}_c)$. This allows the model to learn task-specific projections from the rich semantic information encoded in \mathbf{v}_c while maintaining computational efficiency by keeping the underlying BGE embeddings fixed during training.

The time-aware attention function $A(\cdot)$ captures both semantic relationships and temporal dependencies:

$$A(Q, K, t) = \text{softmax} \left(\frac{Q^\top K}{\sqrt{d}} w(t) \right) \quad (4)$$

where $w(t)$ is a learnable temporal weighting function

$$w(t) = \sigma(a_0 + a_1 t + a_2 t^2 + \dots + a_s t^s)$$

Here, $\{a_0, \dots, a_s\}$ are learnable coefficients for $w(t)$, and σ is a sigmoid ensuring temporal weights are within $[0, 1]$ for stability. The polynomial design of $w(t)$ offers a flexible and interpretable framework for modeling temporal influence. Our ablation studies (Section 6) confirm that the polynomial basis (Order 5) provides a strong balance of expressiveness, structured modeling, and efficiency for nuanced temporal dependency capture, outperforming simpler (piecewise) or comparably performing but more computational cost (MLP) alternatives.

This time-aware attention mechanism effectively captures both semantic relationships and temporal dependencies among clinical events. By dynamically adjusting influence based on temporal proximity, it establishes a robust foundation for handling complex temporal patterns in patient histories.

3.2 Multi-scale Temporal Representation

Clinical events exhibit intricate temporal dependencies across varying time scales. For example, a patient’s current condition might be influenced by both recent medications and chronic diseases diagnosed years ago. Furthermore, the irregularity in the timing and number of historical events across patients introduces additional challenges. To address these complexities, we construct a unified representation of patient history, $\mathbf{h}_t^{(i)}$, using a hierarchical attention mechanism:

$$\mathbf{h}_t^{(i)} = \sum_{j=1}^m \alpha_j(t) E_{c_j}(t),$$

where $m = |\mathcal{H}_t^{(i)}|$ is the number of events before time t for patient i .

The attention weights $\alpha_j(t)$ incorporate both semantic relevance and temporal proximity:

$$\alpha_j(t) = \frac{\exp((Q_{\text{base}}^\top E_{c_j}(t))w(|t - t_j|))}{\sum_{k=1}^m \exp((Q_{\text{base}}^\top E_{c_k}(t))w(|t - t_k|))}.$$

Here, Q_{base} is a learnable query vector optimized to identify historically relevant events, and the learned temporal weighting function $w(|t - t_{k,j}|)$ adjusts event influence based on temporal distance. This allows the model to prioritize clinically significant events while modulating their relevance by time, with softmax normalization enabling focus on multiple relevant events simultaneously.

This temporal attention mechanism provides several critical capabilities: it captures both fine-grained intra-visit and long-term inter-visit temporal patterns (e.g., sequential ordering, chronic disease progression), effectively handles irregular temporal intervals common in clinical data, learns disease progression dynamics across diverse time scales, and models complex interactions among co-occurring medical conditions, including simultaneous and temporally dependent events.

Through this mechanism, the unified representation $\mathbf{h}_t^{(i)}$ encodes a patient’s comprehensive health state at time t , capturing both temporal patterns and clinical relationships. Beyond predicting visit timing and codes, $\mathbf{h}_t^{(i)}$ can be leveraged for various downstream clinical predictions, including disease onset and other health outcomes.

3.3 Joint Training Objective

The model is trained to predict both the timing and medical codes of future visits through (1) and (2), where functions g and f are implemented as multilayer perceptrons with GELU activation. Specifically, both networks first project demographic features and history representations into lower-dimensional spaces independently through single hidden layers, then concatenate and process them through fully connected layers, a 4-layer network for g to output the intensity value and a 3-layer network for f to predict code probabilities.

3.3.0.1 Temporal Point Process Loss. To model visit time, we minimize a least-squares functional derived from empirical risk minimization principles (Geer, 2000; Massart, 2007; Koltchinskii, 2011; Bartlett and Mendelson, 2006):

$$\mathcal{L}_{\text{time}}(\theta) = \|\lambda_\theta\|_T^2 - \frac{2}{T} \int_{[0,T]} \lambda_\theta(t) dN(t),$$

where $\|\lambda_\theta\|_T^2$ denotes the squared norm of the intensity function, and the second term measures the model’s fit at event times. By the Doob-Meyer decomposition, this loss is minimized when λ_θ converges to the true intensity function.

Using Monte Carlo sampling, the squared norm term is approximated as:

$$\|\lambda_\theta\|_T^2 = \frac{1}{T} \int_{[0,T]} \lambda_\theta(t)^2 dt \approx \frac{1}{N} \sum_{i=1}^N \lambda_\theta(t_i)^2,$$

where t_i are time points uniformly sampled from the interval $[0, T]$, and N is the number of samples used to approximate the integral. The second term is computed using the observed event times:

$$\frac{2}{T} \int_{[0,T]} \lambda_\theta(t) dN(t) = \frac{2}{T} \sum_{(t_j, c_j) \in \mathcal{H}_t} \lambda_\theta(t_j).$$

3.3.0.2 Clinical Code Prediction Loss. To address the inherent class imbalance in clinical code prediction, we adopt a focal loss:

$$\mathcal{L}_{\text{code}} = - \sum_{c \in \mathcal{C}} \alpha (1 - p_c)^\gamma \tilde{y}_c \log(p_c),$$

where p_c is the predicted probability for code c , and \tilde{y}_c is the smoothed ground truth label (0.95 for positive cases and 0.05 for negative cases). The parameters $\alpha = 0.25$ and $\gamma = 2.0$ are standard choices that balance the loss contributions and emphasize harder examples. This dynamic adjustment ensures that the model focuses on rare, misclassified examples.

The combined loss function for joint optimization is $\mathcal{L} = \mathcal{L}_{\text{time}} + \gamma \mathcal{L}_{\text{code}}$, where γ is a hyperparameter balancing the temporal and clinical prediction tasks. This joint optimization framework enables the model to learn both temporal patterns and clinical relationships, providing a holistic understanding of a patient’s healthcare trajectory.

3.4 Fine-tuning for Downstream Tasks

After pre-training our model on the temporal point process objectives, we fine-tune it for downstream clinical prediction tasks including disease onset prediction. For each task k , the model processes 1024 clinical events before the target event (e.g., the first occurrence of a disease) to generate the corresponding history representation $\mathbf{h}_t^{(i)}$ and predict the outcome through task-specific MLPs: $p_k^{(i)} = \text{MLP}_k(\mathbf{h}_t^{(i)})$, where $p_k^{(i)}$ represents the predicted probability for task k . The model is trained using weighted binary cross-entropy loss to handle class imbalance:

$$\mathcal{L}_{\text{task}} = - \sum_{i=1}^N w_k [y_k^{(i)} \log(p_k^{(i)}) + (1 - y_k^{(i)}) \log(1 - p_k^{(i)})],$$

where w_k is the task-specific weight. To preserve the temporal patterns learned during pre-training, we employ a differential learning rate strategy, applying a lower learning rate for pre-trained parameters and a higher rate for task-specific layers. Finally, we summarize the procedure in Algorithm 1 in Appendix A.

4 Experiments

4.1 Dataset and Preprocessing

We evaluate TALE-EHR on two distinct EHR datasets: the large-scale adult MIMIC-IV database (Johnson et al., 2023) (inpatient, ICU, emergency visits; including diagnoses, medications, procedures, labs) and the Paediatric Intensive Care (PIC) database (Zeng et al., 2020) (paediatric ICU data; similar clinical information extracted).

Our preprocessing pipeline standardizes both datasets. A roll-up strategy aggregates lower-level medical codes into higher-level categories (diagnoses, medications, procedures, labs) to reduce sparsity and improve comparability, ensuring appropriate granularity (MIMIC-IV roll-up details in Appendix C). For temporal encoding, event timestamps are converted to relative distances from the patient’s initial record ($t = 0$), normalized to a consistent unit (e.g., weeks), and then logarithmically transformed to handle large variations.

The processed MIMIC-IV dataset contains 12,232 unique codes from 342,917 patient records; the PIC dataset yields 2,607 codes from 12,868 records. Both datasets are partitioned into 70% training, 10% validation, and 20% testing sets.

4.2 Training Procedure

Training is two-stage. Pre-training (Section 3.3) learns temporal point process objectives for 10 epochs (Adam, LR 10^{-4} , batch 16). Fine-tuning (Section 3.4) then adapts the model for disease and clinical benchmark prediction. During fine-tuning, most pre-trained parameters are frozen, except for the trainable time-weighting network and base query layers; their learning rate is reduced to 10^{-5} for stability. Disease-specific classifiers are trained for 5 epochs using identical optimization settings.

4.3 Evaluation Metrics

For medical code prediction (next visit), we report $\text{Acc}@K$ ($K = 5, 10, 20$), macro F1-score, and Recall (details in Appendix E). For disease prediction and clinical benchmark tasks, we use AUROC, AUPRC, and F1-score to assess classification effectiveness and the model’s ability to correctly identify disease occurrences while mitigating errors.

4.4 Baseline Models

TALE-EHR is compared against several models for EHR modeling. The baseline models include: LSTM (Hochreiter and Schmidhuber, 1997), Retain (Choi et al., 2016), a recurrent attention model that improves interpretability by assigning weights to past visits. RetainEx (Kwon et al., 2018), an extension of Retain that enhances interpretability by incorporating additional structured medical information. Dipole (Choi et al., 2016), a bidirectional recurrent neural network (RNN) that captures temporal dependencies in patient trajectories. HiTANet (Li et al., 2022), a hierarchical Transformer-based model that introduces time-aware attention mechanisms for clinical event prediction. Cehr_Bert (Pang et al., 2021), which employs a hybrid strategy for temporal modeling by inserting discrete "Artificial Time

Tokens" between visits and concatenating time2vec-generated time and age embeddings with concept embeddings as input to a BERT architecture.

Table 1: Performance Comparison on Disease Prediction (MIMIC-IV)

Model	Arteriosclerosis			Type 2 Diabetes			Hyperlipidemia		
	AUROC	AUPRC	F1	AUROC	AUPRC	F1	AUROC	AUPRC	F1
LSTM	0.841±.007	0.553±.009	0.597±.008	0.848±.007	0.623±.009	0.646±.011	0.816±.003	0.629±.005	0.631±.013
Retain	0.891±.005	0.641±.011	0.639±.009	0.887±.005	0.656±.008	0.676±.009	0.825±.009	0.633±.015	0.653±.011
RetainEX	0.907±.004	0.688±.008	0.601±.012	0.908±.004	0.693±.010	0.637±.013	0.850±.006	0.673±.012	0.646±.011
Dipole	0.895±.007	0.618±.011	0.591±.013	0.873±.006	0.641±.012	0.626±.013	0.832±.009	0.656±.014	0.631±.010
HiTANet	0.909±.006	0.781±.006	0.682±.007	0.919±.004	0.777±.007	0.668±.008	0.909±.004	0.781±.006	0.682±.007
Cehr_Bert	0.912±.004	0.790±.007	0.694±.007	0.924±.005	0.785±.007	0.688±.009	0.915±.003	0.792±.007	0.693±.008
TALE-EHR	0.939±.005	0.811±.006	0.744±.006	0.941±.004	0.813±.008	0.743±.011	0.931±.004	0.833±.005	0.741±.009
Model	Depression			Gastroesophageal Reflux			Acute Kidney Injury		
	AUROC	AUPRC	F1	AUROC	AUPRC	F1	AUROC	AUPRC	F1
LSTM	0.822±.009	0.529±.007	0.532±.011	0.782±.007	0.611±.010	0.488±.010	0.871±.006	0.581±.013	0.509±.011
Retain	0.817±.003	0.519±.009	0.541±.009	0.834±.006	0.621±.006	0.534±.008	0.880±.006	0.613±.010	0.537±.008
RetainEX	0.848±.011	0.536±.014	0.595±.017	0.793±.003	0.611±.007	0.536±.012	0.867±.004	0.695±.008	0.561±.008
Dipole	0.824±.006	0.587±.011	0.521±.013	0.818±.002	0.602±.009	0.528±.011	0.897±.005	0.624±.012	0.608±.007
HiTANet	0.838±.007	0.610±.009	0.545±.011	0.856±.005	0.644±.006	0.508±.009	0.938±.007	0.628±.007	0.597±.013
Cehr_Bert	0.840±.008	0.612±.008	0.551±.009	0.857±.004	0.657±.007	0.510±.012	0.941±.008	0.631±.010	0.601±.013
TALE-EHR	0.878±.005	0.637±.008	0.598±.010	0.891±.005	0.698±.008	0.604±.007	0.961±.005	0.670±.012	0.649±.011
Model	Atrial Fibrillation			Heart Failure			Hypertension		
	AUROC	AUPRC	F1	AUROC	AUPRC	F1	AUROC	AUPRC	F1
LSTM	0.853±.007	0.503±.011	0.519±.014	0.847±.004	0.528±.007	0.490±.017	0.858±.005	0.710±.009	0.627±.008
Retain	0.876±.006	0.569±.006	0.555±.010	0.870±.003	0.541±.006	0.538±.008	0.886±.005	0.727±.012	0.663±.009
RetainEX	0.867±.007	0.506±.009	0.504±.010	0.874±.004	0.543±.007	0.533±.013	0.919±.008	0.764±.008	0.683±.012
Dipole	0.874±.005	0.531±.006	0.537±.008	0.902±.006	0.566±.010	0.570±.015	0.879±.003	0.756±.006	0.658±.013
HiTANet	0.922±.005	0.560±.007	0.571±.008	0.897±.004	0.563±.006	0.575±.013	0.909±.006	0.782±.009	0.681±.014
Cehr_Bert	0.921±.007	0.562±.009	0.573±.011	0.905±.006	0.567±.008	0.574±.013	0.911±.008	0.778±.011	0.684±.016
TALE-EHR	0.931±.002	0.630±.005	0.622±.004	0.938±.003	0.661±.009	0.643±.012	0.931±.005	0.812±.006	0.727±.010

5 Results and Discussion

5.1 Disease and Common Clinical Benchmark Prediction

Table 1 presents classification performance for nine representative diseases, where TALE-EHR achieves the highest scores for all diseases, demonstrating superior generalization. TALE-EHR’s explicit temporal modeling and history representation enable accurate disease classification across diverse conditions, making it highly applicable for real-world clinical settings. For instance, rapid decay for acute conditions and more gradual decay for chronic ones, as detailed in Appendix D. Table 2 summarizes the results on two common clinical benchmarks. TALE-EHR consistently outperforms all baseline models across AUROC, AUPRC, and F1-score for both benchmark tasks. These results further confirm the effectiveness of TALE-EHR for diverse clinical prediction tasks built upon longitudinal EHR data.

5.2 Generalization to Paediatric Data (PIC)

To assess generalizability beyond adult populations, TALE-EHR was evaluated on the Paediatric Intensive Care (PIC) dataset (Zeng et al., 2020) across four relevant paediatric ICU tasks: Pneumonia, Heart Malformations, in-hospital Mortality, and ICU length of stay >7 days. As shown in Table 3, TALE-EHR consistently outperformed baseline models

Table 2: Performance on Clinical Benchmark Tasks (MIMIC-IV)

Model	Hospital 30-day Readmission			LOS > 7 days (next visit)		
	AUROC	AUPRC	F1	AUROC	AUPRC	F1
LSTM	0.736±.003	0.419±.002	0.442±.009	0.724±.002	0.177±.005	0.227±.001
Retain	0.710±.004	0.427±.011	0.443±.004	0.740±.003	0.184±.002	0.244±.011
RetainEX	0.734±.012	0.478±.007	0.447±.003	0.743±.009	0.185±.005	0.247±.017
Dipole	0.739±.002	0.496±.003	0.477±.005	0.745±.006	0.192±.008	0.265±.012
HiTANet	0.754±.005	0.512±.009	0.522±.004	0.750±.004	0.189±.003	0.261±.003
Cehr_Bert	0.756±.008	0.515±.006	0.531±.005	0.751±.006	0.185±.007	0.268±.009
TALE-EHR	0.762±.001	0.536±.004	0.563±.002	0.759±.002	0.195±.002	0.278±.003

across all four tasks, achieving the highest AUROC, AUPRC, and F1 scores. This strong performance on PIC data highlights TALE-EHR’s robustness and ability to generalize across different clinical environments, patient populations (paediatric vs. adult), and prediction tasks, underscoring its broad applicability.

Table 3: Performance on PIC Dataset

Model	Pneumonia Prediction			Heart Malformations Prediction		
	AUROC	AUPRC	F1	AUROC	AUPRC	F1
LSTM	0.885±.001	0.463±.003	0.550±.004	0.825±.002	0.206±.005	0.329±.007
Retain	0.912±.002	0.538±.003	0.602±.005	0.856±.003	0.236±.004	0.335±.004
RetainEX	0.902±.006	0.537±.009	0.582±.010	0.867±.005	0.267±.004	0.342±.007
Dipole	0.920±.005	0.559±.007	0.598±.004	0.866±.005	0.253±.006	0.342±.005
HiTANet	0.929±.003	0.568±.007	0.621±.009	0.886±.002	0.310±.002	0.382±.004
Cehr_Bert	0.933±.004	0.573±.011	0.628±.006	0.884±.006	0.313±.005	0.384±.006
TALE-EHR	0.945±.002	0.613±.003	0.651±.006	0.906±.003	0.340±.005	0.409±.005
Model	Mortality Prediction			ICU LOS > 7 days		
	AUROC	AUPRC	F1	AUROC	AUPRC	F1
LSTM	0.894±.004	0.373±.004	0.448±.006	0.841±.003	0.679±.002	0.664±.005
Retain	0.904±.003	0.422±.005	0.450±.008	0.851±.002	0.700±.005	0.665±.006
RetainEX	0.912±.009	0.423±.011	0.451±.006	0.859±.006	0.715±.007	0.683±.008
Dipole	0.913±.006	0.421±.009	0.456±.005	0.863±.001	0.729±.004	0.685±.002
HiTANet	0.921±.004	0.429±.005	0.464±.003	0.874±.002	0.747±.003	0.705±.004
Cehr_Bert	0.923±.003	0.431±.005	0.467±.004	0.877±.004	0.751±.006	0.713±.009
TALE-EHR	0.934±.002	0.443±.005	0.475±.004	0.897±.001	0.784±.002	0.741±.004

6 Ablation Study

The ablation study systematically evaluates key design choices within TALE-EHR, focusing on: (1) the temporal encoding strategy, (2) the impact of the time-aware mechanism, and (3) the contribution of the embedding initialization approach. Through these experiments, we aim to validate our model design choices and understand their individual contributions to overall disease prediction performance. We consider the following model variants, with results presented in Table 4:

Table 4: Ablation Study Results on Disease Prediction evaluated using AUROC.(MIMIC-IV)

Disease	Poly=5	MLP	Poly=10	Piecewise	W/O time	Random Embed
Arteriosclerosis	0.939±.005	0.937±.006	0.934±.004	0.922±.007	0.911±.008	0.927±.010
Type 2 Diabetes	0.941±.004	0.942±.006	0.937±.006	0.927±.006	0.919±.008	0.931±.007
Hyperlipidemia	0.931±.004	0.928±.005	0.925±.006	0.919±.006	0.912±.003	0.922±.006
Depression	0.878±.005	0.875±.007	0.870±.006	0.859±.005	0.844±.009	0.863±.009
Gastroesophageal Reflux	0.891±.005	0.889±.004	0.882±.008	0.869±.003	0.852±.005	0.873±.012
Acute Kidney Injury	0.961±.005	0.964±.005	0.957±.004	0.948±.007	0.938±.003	0.956±.010
Atrial Fibrillation	0.931±.002	0.930±.004	0.927±.006	0.923±.005	0.914±.006	0.925±.013
Heart Failure	0.938±.003	0.936±.005	0.930±.004	0.921±.003	0.902±.008	0.931±.008
Hyperlipidemia	0.931±.005	0.932±.004	0.927±.006	0.919±.005	0.908±.004	0.925±.009

- **Polynomial Basis (Order 5) [Ours, Poly=5]**: Our main TALE-EHR model, learns the time-aware representations within the attention mechanism using a polynomial function of degree 5.
- **MLP for Time-Awareness [MLP]**: Replaces the polynomial basis function with an MLP to learn the time-aware representations within the attention mechanism.
- **Polynomial Basis (Order 10) [Poly=10]**: Extends the polynomial function to degree 10 to assess the impact of increased temporal expressiveness.
- **Piecewise Function for Time Encoding [Piecewise]**: Employs a predefined set of 7 discrete time intervals (1-7 days, 7-30 days, 30-90 days, 90-180 days, 180-365 days, 365-720 days, and >720 days) to represent time, implemented as indicator functions.
- **Without Time-Aware Mechanism [W/O time]**: Removes the explicit time-aware component from TALE-EHR, forcing the model to rely solely on sequence order without explicit temporal distance modeling. This variant still uses LLM-derived embeddings.
- **Random Initialized Embedding [Random Embed]**: Replaces LLM-derived embeddings with random ones, retaining Poly=5 time-awareness, to isolate pre-trained knowledge contribution.

Table 4 presents AUROC scores for these variants. Our TALE-EHR with Polynomial Basis (Order 5) demonstrates strong performance. An MLP-based time-awareness variant yields comparable efficacy, However, Poly=5 was selected for its balance of performance and structured efficiency. Increasing the polynomial order to 10 slightly degrades performance, likely due to overfitting or increased sensitivity to minor temporal variations. A Piecewise Function approach shows a more noticeable decline, suggesting predefined intervals lack flexibility for nuanced temporal dependencies. The critical role of the time-aware mechanism is highlighted by the "W/O time aware" variant. Lacking explicit temporal modeling, its performance drops significantly across all diseases, underscoring that explicitly modeling temporal relationships is paramount for effective clinical event sequence modeling.

Finally, comparing Poly=5 with LLM embeddings to a variant with Random Initialized Embeddings (which retains Poly=5 time encoding) assesses the impact of pre-trained knowledge. While the random embedding model performs respectably, it consistently underperforms its LLM-equipped counterpart and exhibits increased result variance. This

confirms LLM embeddings enhance predictive accuracy and stability. Notably, the performance gains from the time-aware mechanism itself are more substantial than those lost by switching from LLM to random embeddings. This suggests that while LLM embeddings offer a significant advantage, the sophisticated time-aware architecture is the primary driver of TALE-EHR’s strong performance.

These findings validate our design choices: TALE-EHR, with polynomial time representations (Order 5) and augmented by pre-trained LLM embeddings, offers a robust, high-performing EHR modeling framework. The study emphasizes the foundational importance of the explicit time-aware mechanism, with LLM embeddings serving as a powerful performance and stability enhancer.

7 Conclusion

We introduced TALE-EHR, a novel framework synergistically integrating sophisticated time-aware attention with rich semantic understanding from pre-trained LLM embeddings, significantly enhancing EHR modeling. Extensive experiments show TALE-EHR effectively captures intricate clinical dependencies, consistently outperforming state-of-the-art baselines in medical code and diverse disease prediction tasks. Evaluations on MIMIC-IV and PIC datasets confirm its superior predictive accuracy, especially for complex conditions requiring nuanced interpretation of long-term patient context. Comprehensive ablation studies rigorously underscore the indispensable role of its explicit, continuous temporal modeling. By fusing advanced temporal modeling with deep pre-trained medical knowledge, TALE-EHR advances EHR analytics, paving the way for more reliable real-world clinical decision-making support. Future work includes extending this framework to incorporate multimodal data, like clinical notes and imaging, for a more holistic patient understanding.

References

- Bartlett, P. L. and S. Mendelson (2006, Jul). Empirical minimization. *Probability Theory and Related Fields* 135(3), 311–334.
- Chen, J., C. Liu, J. Sun, S. Saria, and H. Xue (2020). Modeling inter-dependence between time and mark in multivariate temporal point processes. *Journal of Machine Learning Research* 21(171), 1–38.
- Chen, J., S. Xiao, P. Zhang, K. Luo, D. Lian, and Z. Liu (2024). Bge m3-embedding: Multilingual, multi-functionality, multi-granularity text embeddings through self-knowledge distillation. *arXiv preprint arXiv:2402.03216*.
- Choi, E., M. T. Bahadori, J. A. Kulas, A. Schuetz, W. F. Stewart, and J. Sun (2017). Retain: An interpretable predictive model for healthcare using reverse time attention mechanism.
- Choi, E., M. T. Bahadori, A. Schuetz, W. F. Stewart, and J. Sun (2016). Doctor ai: Predicting clinical events via recurrent neural networks. In *Machine Learning for Healthcare (MLHC)*.
- Choi, E., M. T. Bahadori, D. Sontag, and J. Li (2016). Learning the joint representation of heterogeneous temporal events for clinical endpoint prediction. In *Proceedings of the AAAI Conference on Artificial Intelligence*, Volume 30.
- Choi, E., M. T. Bahadori, J. Sun, J. Kulas, A. Schuetz, and W. Stewart (2016). Retain: An interpretable predictive model for healthcare using reverse time attention mechanism. *Advances in neural information processing systems* 29.
- Choi, S., H. J. Kim, J. Lee, and et al. (2020). Using transformer models to predict clinical events in electronic health records. *Proceedings of the 2020 IEEE International Conference on Healthcare Informatics (ICHI)*, 290–295.
- Daley, D. J. and D. Vere-Jones (2003). *An introduction to the theory of point processes: volume I: elementary theory and methods*. Springer.
- Du, N., H. Dai, R. Trivedi, U. Upadhyay, M. Gomez-Rodriguez, and L. Song (2016). Recurrent marked temporal point processes: Embedding event history to vector. In *Proceedings of the 22nd ACM SIGKDD international conference on Knowledge Discovery and Data Mining*, pp. 1555–1564.
- Geer, S. (2000). *Empirical Processes in M-Estimation*. Cambridge Series in Statistical and Probabilistic Mathematics. Cambridge University Press.
- Hochreiter, S. and J. Schmidhuber (1997). Long short-term memory. *Neural Computation* 9(8), 1735–1780.
- Hur, K., J. Lee, J. Oh, W. Price, Y.-H. Kim, and E. Choi (2022). Unifying heterogeneous electronic health records systems via text-based code embedding.

- Johnson, A. E., L. Bulgarelli, L. Shen, A. Gayles, A. Shammout, S. Horng, T. J. Pollard, S. Hao, B. Moody, B. Gow, et al. (2023). MIMIC-IV, a freely accessible electronic health record dataset. *Scientific data* 10(1), 1.
- Kim, J., C. Shim, B. S. K. Yang, C. Im, S. Y. Lim, H.-G. Jeong, and E. Choi (2024). General-purpose retrieval-enhanced medical prediction model using near-infinite history.
- Koltchinskii, V. (2011). *Oracle Inequalities in Empirical Risk Minimization and Sparse Recovery Problems: École d'Été de Probabilités de Saint-Flour XXXVIII-2008*. Lecture Notes in Mathematics. Springer Berlin, Heidelberg.
- Kwon, B. C., H. Park, J. Soman, J. Sun, and H. Park (2018). Retainex: Interpretable ehr document representation for clinical predictions. In *Proceedings of the 24th ACM SIGKDD International Conference on Knowledge Discovery & Data Mining (KDD '18)*, pp. 1245–1254. ACM.
- Lample, G., A. Conneau, and et al. (2019). Neural architectures for named entity recognition. *Proceedings of the 2019 International Conference on Natural Language Processing*, 292–300.
- Lee, J. W., S. Amin, A. Amini, and et al. (2020). Transformers for patient data: A deep learning approach to time-series medical records. *arXiv preprint arXiv:2004.03873*.
- Lee, S. A., S. Jain, A. Chen, K. Ono, J. Fang, A. Rudas, and J. N. Chiang (2024). Emergency department decision support using clinical pseudo-notes.
- Li, B., C. Zhou, Z. Wei, and et al. (2019). Knowledge graph embedding for predicting healthcare events. *Proceedings of the 2019 International Joint Conference on Artificial Intelligence*, 3587–3594.
- Li, S., J. Jin, W. Song, L. Zhang, and B. Wu (2022). Hitanet: Hierarchical time-aware attention networks for risk prediction on electronic health records. *IEEE Journal of Biomedical and Health Informatics* 26(4), 1680–1691.
- Liu, L. J., V. Ortiz-Soriano, J. A. Neyra, and J. Chen (2022, December). KIT-LSTM: Knowledge-guided time-aware LSTM for continuous clinical risk prediction. In *2022 IEEE International Conference on Bioinformatics and Biomedicine (BIBM)*. IEEE.
- Liu, Y., J. Shang, F. Wang, and J. Sun (2019). Point processes for competing observations with recurrent networks (popcorn): A generative model of ehr data. In *Proceedings of the 28th International Joint Conference on Artificial Intelligence (IJCAI)*.
- Luo, J., M. Ye, C. Xiao, and F. Ma (2020, August). Hitanet: Hierarchical time-aware attention networks for risk prediction on electronic health records. In *Proceedings of the 26th ACM SIGKDD International Conference on Knowledge Discovery & Data Mining, KDD '20*. ACM.
- Ma, F., R. Chitta, J. Zhou, Q. You, T. Sun, and J. Gao (2017, August). Dipole: Diagnosis prediction in healthcare via attention-based bidirectional recurrent neural networks. In *Proceedings of the 23rd ACM SIGKDD International Conference on Knowledge Discovery and Data Mining, KDD '17*, pp. 1903–1911. ACM.

- Massart, P. (2007). *Concentration Inequalities and Model Selection: Ecole d’Eté de Probabilités de Saint-Flour XXXIII-2003*. Lecture Notes in Mathematics. Springer Berlin, Heidelberg.
- Pang, C., X. Jiang, K. S. Kalluri, M. Spotnitz, R. Chen, A. Perotte, and K. Natarajan (2021). Cehr-bert: Incorporating temporal information from structured ehr data to improve prediction tasks.
- Shang, J., Y. Chen, X. Wang, Y. Liu, and J. Sun (2019). Event-based contrastive learning for medical time series. In *Proceedings of the 25th ACM SIGKDD International Conference on Knowledge Discovery & Data Mining*, pp. 2199–2207.
- Shang, J., Y. Chen, X. Wang, Y. Liu, and J. Sun (2021). Interpretable neural temporal point processes for modeling electronic health records. *Artificial Intelligence in Medicine 116*, 102075.
- Steinberg, E., J. A. Fries, Y. Xu, and N. Shah (2024). MOTOR: A time-to-event foundation model for structured medical records. In *The Twelfth International Conference on Learning Representations*.
- Su, X., S. Messica, Y. Huang, R. Johnson, L. Fessler, S. Gao, F. Sahneh, and M. Zitnik (2025). Multimodal medical code tokenizer.
- Wang, S., X. Li, W. Wang, and et al. (2020). Multi-relational knowledge graph embedding for recommendation and predictive tasks in healthcare. *IEEE Transactions on Knowledge and Data Engineering 32*(10), 1913–1925.
- Wang, Z., C. Gao, C. Xiao, and J. Sun (2024). Meditab: Scaling medical tabular data predictors via data consolidation, enrichment, and refinement.
- Wang, Z. and J. Sun (2022). Transtab: Learning transferable tabular transformers across tables.
- Zeng, X., G. Yu, Y. Lu, L. Tan, X. Wu, S. Shi, H. Duan, Q. Shu, and H. Li (2020, January). Pic, a paediatric-specific intensive care database. *Scientific Data 7*(1).
- Zhang, X., W. Wei, H. Li, and et al. (2019). Learning knowledge graph embeddings for predicting drug-target interactions. *IEEE Access 7*, 52677–52686.

Appendix

A Training Algorithm

Algorithm 1 summarizes the training procedure outlined in Section 3, consisting of pre-training on medical event sequences and fine-tuning for disease prediction. The pre-training phase learns structured temporal and semantic representations of clinical events, while fine-tuning optimizes the model for disease-specific predictions.

Algorithm 1 Time-Aware Language Encoder for EHR (TALE-EHR)

Input: Patient histories $\{\mathcal{H}^{(i)}\}$, medical code set \mathcal{C}

Output: Trained model parameters θ

```
1: // Pre-training Phase
2: Initialize model parameters  $\theta$ 
3: for each medical code  $c \in \mathcal{C}$  do
4:    $x_c \leftarrow \text{GetDescription}(c)$  ▷ Map code to standardized description
5:    $\mathbf{v}_c \leftarrow \text{BGE}(x_c)$  ▷ Generate embeddings from pretrain LLM model
6: for epoch = 1 to  $N_{\text{pretrain}}$  do
7:   for each batch  $\mathcal{B}$  do
8:     for each patient history  $\mathcal{H}_t^{(i)}$  in  $\mathcal{B}$  do
9:       Compute code-level representations using time-aware attention
10:      Generate unified history representation  $\mathbf{h}_t^{(i)}$  for current time  $t$ 
11:      Compute temporal and code prediction losses
12:      Update model parameters using combined loss

13: // Fine-tuning Phase for Disease Prediction
14: Initialize task-specific parameters
15: Configure learning rates for pre-trained and new parameters
16: for epoch = 1 to  $N_{\text{finetune}}$  do
17:   for each batch  $\mathcal{B}$  do
18:     // Disease Prediction
19:     Extract histories before disease onset time
20:     Generate pre-onset unified representations and compute disease loss
21:     Update model parameters
22: return Optimized model parameters  $\theta$ 
```

B Code Description Standardization

After basic preprocessing, our code set primarily consists of six types of codes: ICD, RxNorm, Phecode, CCS, DRG, and MIMIC-IV local codes. We processed these codes and obtained their descriptions as follows. For ICD (International Classification of Diseases) codes, we used the descriptions provided in MIMIC-IV, which contains official WHO (<https://www.who.int/standards/classifications/classification-of-diseases>) descriptions

that provide detailed explanations of each diagnosis. For RxNorm medication codes, we employed the standardized drug descriptions from the National Library of Medicine (NLM) (<https://www.nlm.nih.gov/research/umls/rxnorm>). For Phecode (Phenotype Code), we utilized the standardized definitions and descriptions from the PheWAS Catalog (<https://pewascatalog.org>) maintained by Vanderbilt University, which maps clinical phenotypes to ICD codes. For CCS (Clinical Classifications Software) codes, we incorporated the descriptions provided by HCUP (Healthcare Cost and Utilization Project) (<https://hcup-us.ahrq.gov/toolssoftware/ccs/ccs.jsp>) that categorize medical procedures and services into clinically meaningful groups. For DRG (Diagnosis Related Groups) codes, the EHR contains two classification systems: APR-DRG by 3M (<https://www.solventum.com/en-us/home/h/f/b5005024009/>) which incorporates severity and mortality risk scores, and HCFA-DRG by CMS (<https://www.cms.gov/medicare/payment/prospective-payment-systems/acute-inpatient-pps/ms-drg-classifications-and-software>) for Medicare reimbursement. We mapped these codes to descriptions using files provided in MIMIC-IV. Lastly, for local institution-specific codes, we use the institution’s coding manual descriptions.

C Data Integration and Code Roll-up

The data (<https://mimic.mit.edu/docs/>) contains the EHR of 364,627 patients, out of them 94,458 were in the ICU and out of them 205,504 have attended Emergency department(ED). Patients who have been in the ICU tend to relate to much more codes and occurrences than other patients.

These data comes from **hospital tables**: diagnoses_icd, drgcodes, hcpcsevents, labevents, prescriptions, procedures_icd, **ICU tables**: chartevents, inpatientevents, outpatientevents and **ED tables**: medrecon, pyxis, diagnosis.

Some codes from these tables are aggregated into high-level codes. We convert procedure codes, including HCPC, ICD-9, ICD-10-PCS, to CCS codes. Diagnosis codes, including ICD-9 and ICD-10-CM, are grouped to PheCodes. NDC codes are aggregated to RxNorm CUIs. The statistics of these aggregated codes are shown in Table 5.

Table 5: Statistics of aggregated code

Original Code	Source Table	Number of original code	Target code
ICD9/ICD10PCS	procedures_icd	14,911	CCS
HCPCS	hcpcsevents	2,366	CCS
ICD9/ICD10CM	diagnoses_icd/diagnosis	29,933	PheCode
NDC	prescriptions/medrecon/pyxis	12,243	RxNorm

Some ICD codes from diagnoses_icd with high frequency cannot be grouped to PheCode by the mapping table we use, and we still keep them in the dataset. Eventually, we split some codes from Chartevents into several distinguishable codes, because they occur with only a few unique values. Statistics of code occurrences of the final dataset are shown in Table 6.

Table 6: Statistics of final dataset

Code	Source Table	Number of codes	Total freq	Mean freq	Median freq	Max freq
Chart code	chartevents	1,891	414,200,715	219,037	16,078	12,869,833
Input code	inpuvents	327	10,953,713	33,497	2,300	1,578,656
Output code	outpuvents	66	5,359,187	81,199	8,782	3,599,702
Proc code	procedureevents	159	808,706	5,086	501	101,294
Lab code	labevents	734	158,084,819	215,374	5,779	4,331,615
ICD10	diagnoses_icd/diagnosis	1830	242,533	132	4	33,113
ICD9	diagnoses_icd/diagnosis	954	253,908	266	10	12,600
PheCode	diagnoses_icd/diagnosis	1,793	6,766,921	3,774	557	237,879
DRG	drgcodes	1,087	761,856	700	267	12,633
CCS	hpcps/proc_icd*	234	1,041,681	4,451	1.587	157,740
RxNorm	prescriptions/medrecon	3,157	20,890,607	6,617	30	1,048,814
Total	-	12,232	619,364,646	50,634	222	12,869,833

*CCS codes are derived from hpcsevents and procedures_icd.

D Temporal Weight Analysis

To gain deeper insights into how TALE-EHR models temporal influence, we analyze the learned temporal weighting function $w(\Delta t)$ for different downstream disease prediction tasks. Figure 2 visualizes these learned weighting functions, revealing distinct characteristics based on the nature of the diseases.

First, the analysis highlights Disease-Specific Decay Rates, where the temporal weight decay varies significantly across different diseases. For instance, the curve associated with Acute Kidney Injury (an acute condition, represented by the red line in Figure 2) exhibits rapid decay. This indicates that very recent clinical events hold substantially higher importance for predicting acute illnesses, and the influence of past events diminishes quickly.

Second, a Gradual Decay for Chronic Conditions is observed. In contrast to acute conditions, the weighting functions for chronic conditions like Type 2 Diabetes (green line in Figure 2) and Heart Failure (purple line in Figure 2) show a much more gradual decay. This suggests that for chronic diseases, historical events, even those occurring further in the past, retain a more significant and prolonged influence, reflecting the model’s recognition of their long-term, cumulative impact.

Finally, a Long-Tail Effect for Capturing Distant Influences is notable. Even for diseases with slower decay patterns, the weights do not abruptly drop to zero but instead exhibit a long-tail effect. This implies that very distant events can still maintain small but non-zero weights, allowing the model to capture rare but potentially significant long-term clinical patterns or risk factors that might be relevant much later.

These observations collectively demonstrate that TALE-EHR’s time-aware mechanism capably learns and adapts disease-specific temporal dependencies. It effectively captures the varying importance of events over time, differentiating between the acute, rapidly evolving nature of some conditions and the chronic, long-term influence patterns of others. This adaptability is crucial for building accurate and clinically relevant predictive models from EHR data.

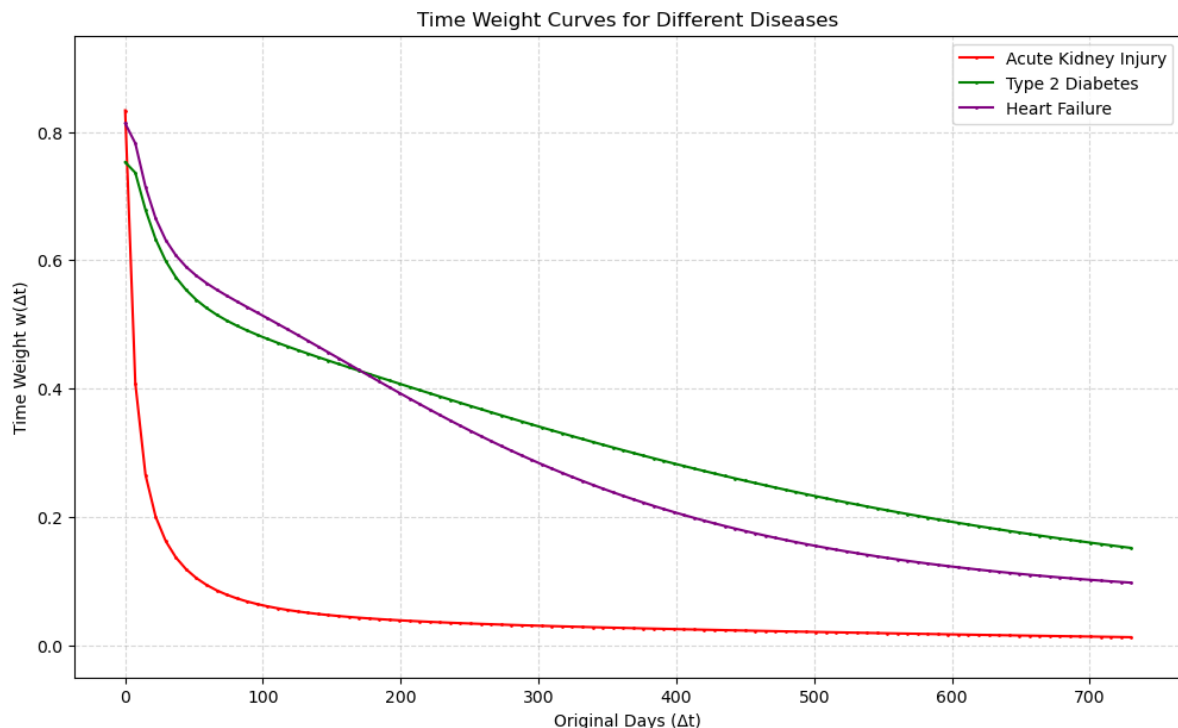


Figure 2: Learned temporal weighting function $w(\Delta t)$ for downstream disease prediction tasks. The x-axis represents the time interval between clinical events (in days), and the y-axis shows the attention weight. The curve demonstrates how the model modulates attention across different temporal scales, with a gradual decay indicating that both recent and historical events contribute to disease prediction, though with decreasing importance over time.

Table 7: Performance in Medical Code Prediction(MIMIC-IV)

Model	Acc@5	Acc@10	Acc@20	F1	Recall
LSTM	0.829±.004	0.824±.003	0.803±.004	0.718±.006	0.627±.009
Retain	0.869±.002	0.861±.004	0.842±.007	0.755±.005	0.667±.023
RetainEx	0.882±.003	0.879±.006	0.830±.010	0.844±.008	0.615±.015
Dipole	0.869±.004	0.862±.004	0.834±.004	0.730±.004	0.673±.011
HiTANet	0.861±.004	0.817±.008	0.787±.009	0.684±.007	0.626±.013
Cehr_Bert	0.881±.003	0.878±.006	0.848±.009	0.842±.008	0.668±.010
TALE-EHR	0.902±.003	0.896±.005	0.862±.006	0.850±.004	0.675±.007

E Medical Code Prediction

Table 7 presents the performance of various models on the medical code prediction task using the MIMIC-IV dataset. TALE-EHR consistently and significantly outperforms all baseline models across all evaluated metrics, achieving top scores in Acc@5 (0.902), Acc@10 (0.896), Acc@20 (0.862), F1-score (0.850), and Recall (0.675). This demonstrates its superior

capability in modeling complex medical code dependencies and accurately predicting a comprehensive set of future codes. Among the baseline models, Cehr_Bert consistently demonstrates robust performance across the Acc@K metrics (e.g., Acc@5: 0.881, Acc@20: 0.848), making it one of the strongest baselines. This may be attributed to BERT’s inherent masked language modeling pre-training, which often aids in predictive tasks. However, TALE-EHR still surpasses Cehr_Bert in all aspects, particularly in F1-score and Recall. RetainEx exhibits a strong start, achieving high scores in Acc@5 (0.882) and a competitive F1-score (0.844), second only to TALE-EHR in the latter. This suggests effectiveness in short-term predictions. However, its performance notably degrades for longer-range predictions (Acc@20 drops to 0.830) and, critically, it records the lowest Recall (0.615) among all compared models. This indicates a significant weakness in capturing a comprehensive set of relevant future codes, especially as the prediction horizon extends. In contrast, TALE-EHR maintains superior accuracy and recall even for larger K. Other models like Retain and Dipole show competitive scores in specific metrics (e.g., Dipole’s Recall at 0.673 is strong among baselines), but none match the consistent, across-the-board superiority of TALE-EHR. HiTANet generally underperforms in this task. The leading F1-score (0.850) and Recall (0.675) achieved by TALE-EHR are particularly noteworthy. A high Recall is crucial in medical applications as it signifies a lower rate of false negatives, meaning fewer actual subsequent medical codes are missed. The high F1-score indicates an excellent balance between precision and recall, making TALE-EHR robust, especially when dealing with the often imbalanced nature of medical code distributions. By effectively integrating its Transformer-based point process framework, TALE-EHR adeptly captures both short- and long-term temporal dependencies inherent in patient visit sequences. This capability translates directly into its superior predictive accuracy across various horizons (K values) and its ability to identify a more complete set of future codes. Consequently, TALE-EHR emerges as a particularly well-suited model for clinical decision-making, where minimizing missed diagnoses and achieving overall predictive accuracy are critical.

F Visualization of Learned Disease Representations

To further investigate the quality of the learned patient history representations $\mathbf{h}_t^{(i)}$, we visualize them using UMAP for several representative diseases from the MIMIC-IV dataset. These visualizations project the high-dimensional history representations into a 2D space, allowing for an intuitive assessment of their separability for disease classification. We compare the representations learned by our TALE-EHR model against those learned by a standard LSTM baseline. In these visualizations, red points denote patients who eventually developed the specific disease (positive cases), while blue points represent patients who did not (negative cases).

Figure 3 displays the UMAP visualizations for disease representations learned by TALE-EHR. Across various diseases, such as Type 2 Diabetes, Arteriosclerosis, and Heart Failure, we observe a discernible separation between the clusters of positive and negative samples. While some overlap is expected due to the inherent complexity and comorbidity in EHR data, the overall clustering trend indicates that TALE-EHR learns representations that are informative for distinguishing between disease outcomes.

In contrast, Figure 4 shows the UMAP visualizations for representations learned by

the LSTM baseline. For many of the same diseases, the separation between positive and negative samples appears less distinct compared to TALE-EHR. The clusters often exhibit more significant overlap, and the overall structure seems less organized with respect to the disease labels.

This qualitative comparison suggests that TALE-EHR’s architecture, particularly its time-aware attention mechanism and integration of rich semantic embeddings, leads to more discriminative patient history representations. The enhanced separability observed in the TALE-EHR visualizations aligns with its superior quantitative performance in disease prediction tasks (as shown in Table 1), providing further evidence of its effectiveness in capturing clinically relevant patterns from complex longitudinal EHR data.

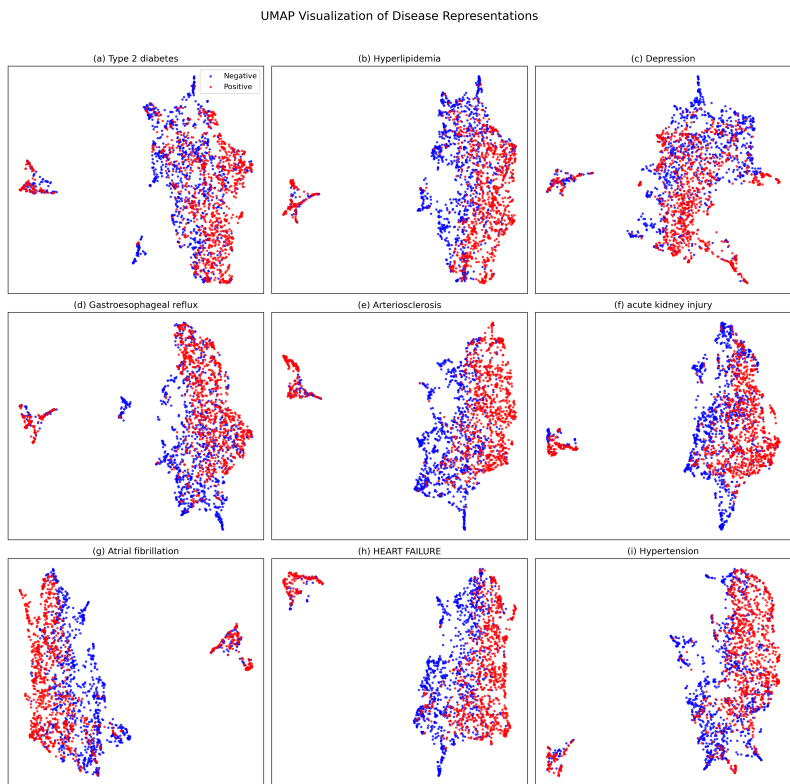


Figure 3: UMAP visualization of disease representations learned by TALE-EHR for nine diseases. Red points indicate positive cases (disease present), and blue points indicate negative cases (disease absent). Clearer separation between red and blue clusters suggests more discriminative representations.



Figure 4: UMAP visualization of disease representations learned by LSTM for the same nine diseases. Comparison with Figure 3 shows generally less distinct separation between positive (red) and negative (blue) cases for LSTM.

Impact Statement

TALE-EHR represents an advancement in EHR modeling by integrating a novel time-aware attention mechanism with strong semantic representations derived from LLM embeddings of standardized code descriptions. This combination significantly improves predictive accuracy for critical clinical tasks such as medical code forecasting and disease progression analysis, as demonstrated by robust performance across diverse datasets (MIMIC-IV and PIC) and standard clinical benchmarks. By more accurately capturing both the complex temporal dynamics and the semantic nuances within patient records, the framework enhances the potential for developing reliable clinical decision support tools. The use of LLM-derived embeddings promotes semantic consistency, contributing to the model's ability to handle varied clinical coding practices effectively. Ultimately, this work could facilitate a deeper understanding of patient trajectories and lead to more dependable outcome predictions, benefiting clinical research and potentially improving patient care pathways.